ARTICLE

Cobalt Ferrite Nanocrystals: Out-Performing Magnetotactic Bacteria

Tanya Prozorov,[†] Pierre Palo,[†,‡] Lijun Wang,[†,‡] Marit Nilsen-Hamilton,[†,‡,*] DeAnna Jones,[†] Daniel Orr,[†,§] Surya K. Mallapragada,[†,§,*] Balaji Narasimhan,[†,§,*] Paul C. Canfield,[†,⊥] and Ruslan Prozorov[†,⊥,*]

[†]Ames Laboratory, U.S. Department of Energy, Ames, Iowa 50011, [‡]Department of Biochemistry, Biophysics and Molecular Biology, [§]Department of Chemical and Biological Engineering, and [⊥]Department of Physics & Astronomy, Iowa State University, Ames, Iowa 50011

ABSTRACT Magnetotactic bacteria produce exquisitely ordered chains of uniform magnetite (Fe_3O_4) nanocrystals, and the use of the bacterial mms6 protein allows for the shape-selective synthesis of Fe_3O_4 nanocrystals. Cobalt ferrite ($CoFe_2O_4$) nanoparticles, on the other hand, are *not* known to occur in living organisms. Here we report on the use of the recombinant mms6 protein in a templated synthesis of $CoFe_2O_4$ nanocrystals *in vitro*. We have covalently attached the full-length mms6 protein and a synthetic C-terminal domain of mms6 protein to self-assembling polymers in order to template hierarchical $CoFe_2O_4$ nanostructures. This new synthesis pathway enables facile room-temperature shape-specific synthesis of complex magnetic crystalline nanomaterials with particle sizes in the range of 40–100 nm that are difficult to produce using conventional techniques.

KEYWORDS: bioinspired synthesis · biomineralization protein · templating · superparamagnetism · magnetic nanocrystals · cobalt ferrite nanocrystals

The synthesis of magnetic nanoparticles with narrow size distribution represents a significant practical and fundamental challenge.[1,2] Such particles are in high demand in various areas, from quantum computing to cancer therapy.[3–12] Contrary to common sense, the smallest nanoparticles are not necessarily the best. Often, larger particles (~50 nm), just below the superparamagnetic threshold, are the most suitable for many applications. For example, in magnetic recording and drug delivery, larger particles with large magnetic moments are preferred.[13–16] The problem is not only the particle size but also significant agglomeration of the particles. It is especially difficult to produce non-agglomerated nanocrystals of ferromagnetic nanoparticles.[17] Various synthetic approaches have been utilized, ranging from homogeneous synthesis[18] to heterogeneous synthesis[2] and to the use of powerful ultrasound to rapidly decompose volatile organometallics.[19–21] One of the drawbacks associated with rapid synthesis is a decreased degree of crystallinity in the resulting material leading, in turn, to a significant spin misalignment, which reduces the total or net magnetic moment per particle. When the synthesis involves a more controlled thermal decomposition, it is possible to somewhat further minimize the crystallinity problems.[1,17]

In this article we describe a novel room-temperature bioinspired route to produce nanocrystals of one of the best known, commercially used ferromagnetic compounds: cobalt ferrite. The idea arose from our investigations of magnetite biomineralization by various magnetotactic bacteria.[22] We investigated the ability of the acidic recombinant protein, mms6, cloned from these bacteria, to promote shape-specific magnetite growth *in vitro*.[23] These experiments were successful and yielded uniform magnetite nanocrystals, resembling those seen in magnetotactic bacteria, as shown in Figure 1.

In addition to replicating nanocrystals seen in nature, we have successfully templated synthesis of more complex and

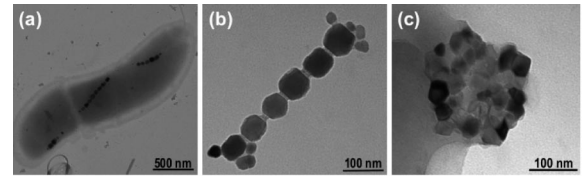

Figure 1. Transmission electron micrographs of (a) *Magnetospirillum magneticum* strain AMB-1 with a chain of magnetosomes inside, (b) nanocrystalline magnetite chain harvested from lysed bacteria (magnetite nanocrystals are held together by a thin phospholipid membrane material after lysis), and (c) protein-templated magnetite nanocrystals of comparable size and morphology. Note the difference in the scale bars.

*Address correspondence to prozorov@ameslab.gov, marit@iastate.edu, nbalaji@iastate.edu, suryakm@iastate.edu.

Received for review August 25, 2007 and accepted September 28, 2007.

Published online October 31, 2007. 10.1021/nn700194h CCC: $37.00

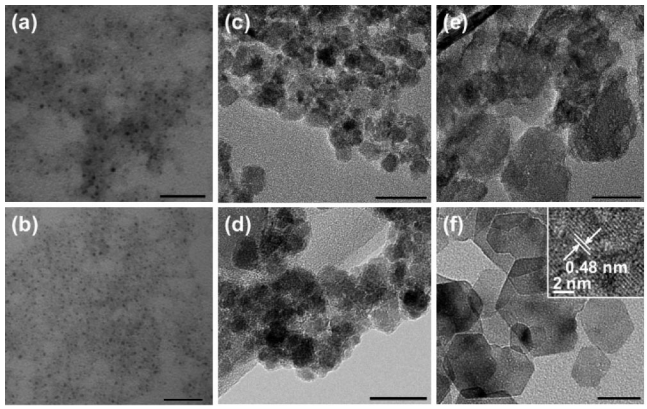

Figure 2. TEM of $CoFe_2O_4$ nanocrystals obtained (a) in protein-free synthesis in Pluronic gel, (b) in protein-free synthesis in Pluronic gel with a small amount of functionalized Pluronic, (c) in the presence of unbound *his*-mms6, (d) in the presence of unbound *c25*-mms6, (e) in the presence of Pluronic-conjugated *his*-mms6, and (f) in the presence of Pluronic-conjugated *c25*-mms6. (Inset) High-resolution (HR) TEM image of a fragment of the central particle with lattice spacing of 0.48 nm between the (111) planes. The scale bar in all images is 50 nm.

highly magnetic nanocrystals that do not occur in living organisms using this bioinspired approach and by investigating a variety of magnetic ions for the synthesis. Here we describe the protein-templated synthesis and characterization of nanostructured cobalt ferrite ($CoFe_2O_4$), which is not known to occur in magnetotactic bacteria. Two forms of mms6 were used in the current study: a recombinant polyhistidine-tagged full-length mms6 (*his*-mms6), and a synthetic C-terminal domain of this protein containing 25 amino acids (*c25*-mms6). To control placement of the formed nanocrystals and minimize nanoparticle aggregation, the two proteins were covalently attached to triblock copolymers, called poloxamers, which hierarchically self-assemble in aqueous solutions to form thermoreversible gels, allowing more controlled diffusion and crystal growth rates.

RESULTS AND DISCUSSION

The ability of *his*-mms6 and *c25*-mms6 to promote shape-selective formation and growth of nanocrystals was tested in a Pluronic gel in the presence of iron and cobalt ions. Figure 2 shows the transmission electron microscopy (TEM) images of $CoFe_2O_4$ nanocrystals obtained in concentrated Pluronic gel without the protein, without the protein in the presence of a functionalized Pluronic block copolymer solution, in the presence of unbound *his*-mms6, in the presence of unbound *c25*-mms6, in the presence of Pluronic-conjugated *his*-mms6, and in the presence of Pluronic-conjugated *c25*-mms6. The small (5–10 nm) particles obtained in the protein-free synthesis (Figure 2a,b) lack specific shape, which points to a poor templating ability of the Pluronic gel alone. Similar to the case of magnetite nanocrystals,[23] 15–20 nm $CoFe_2O_4$ nanocrystals were obtained in the presence of unbound *his*-mms6 (Figure 2c) or unbound *c25*-mms6 (Figure 2d). These nanocrystals exhibited rectangular shapes, most likely due to the protein templating. Finally, nanocrystals synthesized in the presence of either Pluronic-conjugated *his*-mms6 (Figure 2e) or Pluronic-conjugated *c25*-mms6 (Figure 2f) exhibited 50–80 nm thin hexagon-like structures. It can be seen that the nanocrystals in Figure 2f showed more pronounced faceting and more well-defined shapes than those in Figure 2e. The difference in particle shape and size may be attributed to the different templating action of unbound and covalently attached (conjugated) proteins, as discussed below. Under closer examination of the TEM images in Figure 2f, the thin hexagon-like plates appear rather as truncated equilateral triangles. Such nanostructures, therefore, would have a 3-fold symmetry rather than a 6-fold symmetry. Finally, the inset in Figure 2f shows a high-resolution TEM (HRTEM) image of a fragment of the structurally uniform particle (plate) with lattice spacing of approximately 0.48 nm, as will be discussed further.

Figure 3 shows an X-ray powder diffraction pattern of the sample presented in Figure 2f (Cu $K\alpha$; d-spacing, in Å: 5.254, 2.930, 2.52, 2.089, 1.726, 1.477, and 1.605). All diffraction peaks can be indexed to the (111), (220), (311), (400), (422), (333), and (440) planes of spinel $CoFe_2O_4$ with a cubic symmetry (*Fd*3*m*, JCPDS file no. 22-1086) and lattice parameter $a = 8.373(\pm 0.003)$ Å, which is in good agreement with the value of 8.3919 Å reported in JCPDS 22-1086. Chemical impurities were not detected. The relative sharpness of the X-ray diffraction peaks indicates that the material is well crystalline. This is fur-

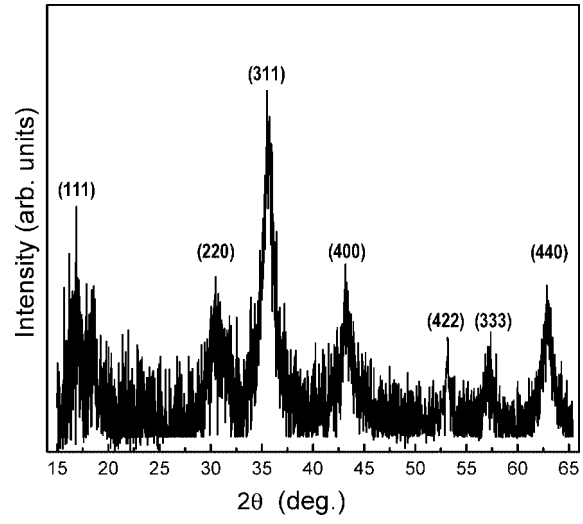

Figure 3. Powder X-ray diffraction pattern of the $CoFe_2O_4$ particles shown in Figure 2f.

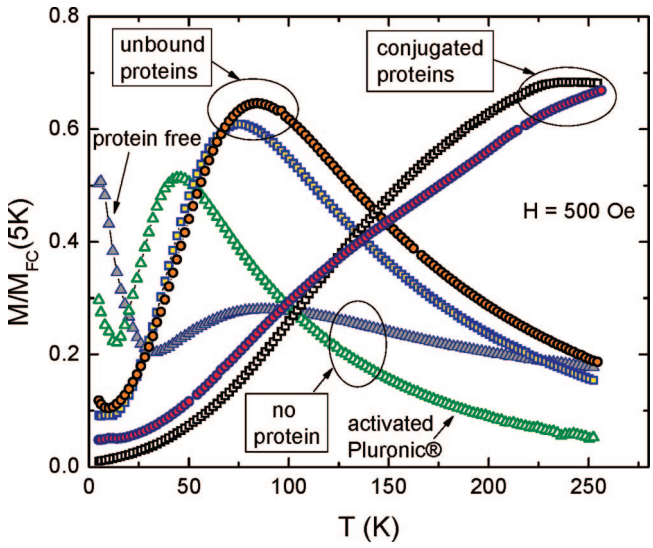

Figure 4. Zero-field-cooled measurements for the six samples discussed in the text. Notice the significant difference in the blocking temperatures between the samples without the biomineralization proteins (Pluronic), with unbound *his*-mms6 and *c25*-mms6 (two middle curves), and with conjugated *his*-mms6 and *c25*-mms6, which have the largest T_B.

ther supported by the high-resolution electron micrograph displayed in the inset of Figure 2f, with 0.48 nm spacing perpendicular to the (111) plane of the plates. This, in turn, corresponds to the nanostructured plates growth along the (111) direction of a cubic cell, therefore having a 3-fold symmetry.

We now turn to a discussion of the magnetic measurements. A ferromagnetic particle becomes "superparamagnetic" below a critical size of the order of 100 nm, depending on the material. Such a particle cannot develop internal magnetic domains and, therefore, acts as a paramagnetic particle with magnetic moment (μ) up to 10^7 Bohr magnetons. The blocking phenomenon (and its characteristic "blocking" temperature, T_B) is a signature of the superparamagnetic regime that depends on the particle size, degree of crystallinity, and interparticle interactions.[24] Below T_B, nanoparticles are "blocked", which means that initially random magnetic moments of individual nanoparticles cannot readily align with the applied field, because magnetic Zeeman (μH) and thermal fluctuation (k_BT) energies are insufficient to overcome the energy barrier set by the magnetic anisotropy and interparticle dipolar interactions. Experimentally, T_B is marked by the peak in the $M(T)$ curve measured upon warming after a magnetic field was applied at a low temperature to a zero-field-cooled sample (so called ZFC-W procedure). It is well established that T_B is reduced for smaller particles and for particles with reduced crystallinity (both leading to the reduction of the magnetic moment per particle).[21,24,25] Another way to probe the magnetic response of superparamagnetic assembly is to measure its magnetic moment at a fixed temperature as a function of the magnetic field. It is important to compare $M(H)$ curves below and above T_B to show the absence of the magnetic hysteresis above T_B. Any residual hysteresis would indicate particle agglomeration, which is an undesired but often observed phenomenon. A detailed discussion of the physics of superparamagnetic nanoparticles is given elsewhere.[24,25]

Figure 4 shows the results of ZFC-W measurements performed upon warming after a magnetic field of 500 Oe was applied at 5 K after cooling in zero applied field. Clearly, nanoparticles grown in the activated Pluronic without proteins exhibit the lowest blocking temperature. Nanoparticles grown in Pluronic gels with either unbound *c25*-mms6 or unbound *his*-mms6 show an elevated T_B. Finally, nanocrystals grown in the presence of Pluronic-conjugated proteins show the largest blocking temperatures. The results are fully consistent with the TEM images, indicating large, well-formed particles grown in the presence of Pluronic-conjugated *his*-mms6 and *c25*-mms6.

Figure 5 compares magnetization loops measured at 5 and 250 K in nanoparticles obtained in the Pluronic gel with and without the Pluronic-conjugated *c25*-mms6.

There is a significant relative reduction in the maximum magnetization at 250 K compared to 5 K in the Pluronic gel alone and only a moderate change in the case of gel with Pluronic-conjugated *c25*-mms6. Also, nanocrystals formed in the presence of Pluronic-conjugated *c25*-mms6 exhibit a very large coercivity field, ~0.9 T at 5 K (compared to 0.5 T for the protein-free Pluronic), and a much larger remnant magnetization, 54% of its value at 5 T (*versus* 25% in Pluronic). Such an enhancement of the irreversible properties is consistent with an elevated blocking temperature in nanocrystals synthesized with Pluronic-conjugated *c25*-

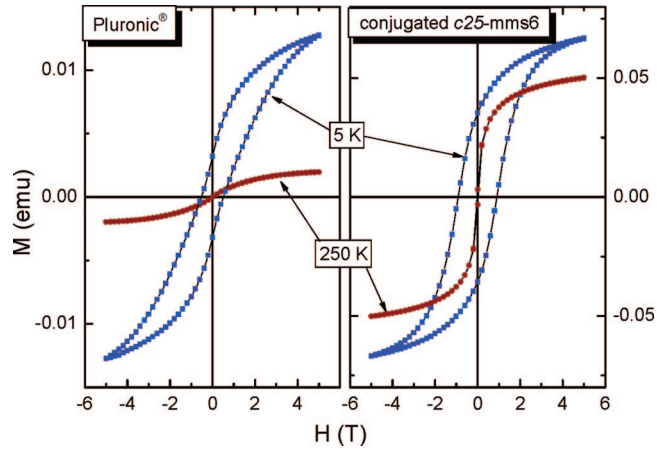

Figure 5. Magnetization loops at 5 and 250 K, measured in nanoparticles obtained in functionalized protein-free Pluronic (left) and with conjugated *c25*-mms6 (right).

mms6. Note, however, that the magnetic hysteresis in both cases is virtually zero at 250 K, which indicates that the nanoparticles are not blocked and are not agglomerated, so the reported enhancement of the irreversibility at low temperatures is intrinsic, and our nanoparticles are superparamagnetic. Finally, the initial susceptibility in this reversible state is much larger in nanoparticles formed with Pluronic-conjugated *c25*-mms6, which is consistent with a much larger effective magnetic moment for a well-shaped larger particle, as seen in the TEM images.

On the basis of all of the above experiments, we offer the following hypothesis on the mechanism of protein-templated nanocrystal formation. The acidic iron-binding mms6 protein was first reported by Arakaki and co-workers as a membrane protein.[26] The hydrophobic N-terminus of this protein is presumed to be closely associated with the magnetosome phospholipid membrane, while the hydrophilic C-terminus is tightly bound to the bacterial magnetic particle. *In vivo*, this protein is likely to form an acidic binding surface lining of the vesicle membrane, thus promoting the formation of the uniform cuboctahedral magnetite nanocrystals.[11,26,27] Moreover, in addition to iron binding activity, mms6 was shown to competitively bind several other metal ions,[26] including Mg^{2+}, Zn^{2+}, Cu^{2+}, and Ni^{2+}. Taking into account the differences in atomic radii and electronic configurations of metal ions, a cavity-controlled, ion-specific binding to the mms6 is implausible. In concentrated Pluronic gels, micelles self-assemble into a variety of hierarchical structures, including the face-centered cubic and body-centered cubit lattices,[28–33] and such arrangement within the gel is likely to affect the shapes of further liquid components. The consequent gelation of Pluronic by hierarchical self-assembly is maintained in the presence of both unbound and Pluronic-conjugated proteins. If, under the current synthetic conditions, the micelles in the amphiphilic Pluronic block copolymers self-assemble into hierarchical architectures,[34–36] they could presumably act in a manner similar to that of the mms6-containing bacterial phospholipid membranes, allowing a surface-controlled crystal growth. Both unbound forms of mms6 are likely to phase-separate from the gel into the water-rich regions of the gels, being expelled from the micelles. Thus, neither unbound *his*-mms6 nor *c25*-mms6 can provide the extended surface needed for the nucleation and growth of larger nanoparticles, as is evident from the analysis of the TEM images shown in Figure 2. By contrast, Pluronic-conjugated forms of mms6 inevitably become incorporated into the micelles and are thus brought into closer contact, with a greater probability of forming extended ion-binding surfaces. Here, the close packing of micelles in the gel appears to stimulate crystal growth along the (111) direction of the cubic cell. We have determined that *his*-mms6 protein forms large aggregates, whereas *c25*-mms6 forms smaller ones.[37] It is likely that aggregation of mms6 affects the crystal formation, with a number of protein molecules assembled into the multimers and enabling formation of sizeable nanocrystals. Steric effects, therefore, are expected to play an important role in this process. Here, the crystal-templating ability of the significantly larger Pluronic-conjugated *his*-mms6 would be inferior to that of the less aggregated and more compact *c25*-mms6, as is clearly reflected in the TEM images shown in Figure 2e,f. These observations are also in complete agreement with the magnetic properties measurements in Figures 3 and 4, suggesting that the Pluronic-conjugated *c25*-mms6 provides controlled crystal sizes and shapes with superior magnetic behavior, which is not achievable using conventional room-temperature synthesis methods.

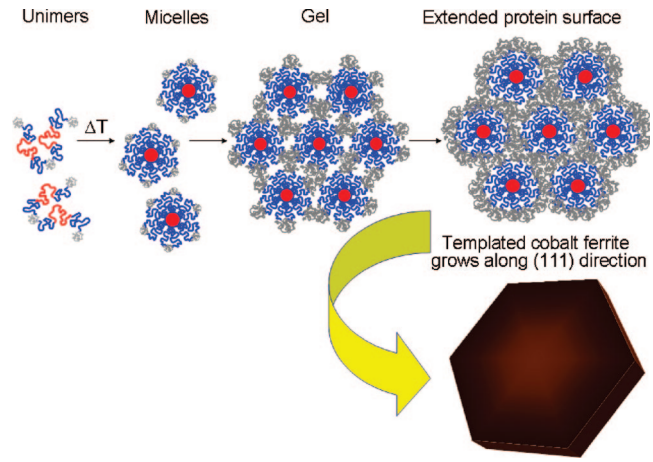

Figure 6. A plausible scenario for the protein-templated synthesis of $CoFe_2O_4$ nanocrystals in the presence of the Pluronic-conjugated recombinant mms6. Here, hexagonal nanoparticles are templated by the protein on hexagonally packed micelles, with the crystal growth along the (111) direction of a cubic cell.

A proposed scenario of the protein-templated synthesis of $CoFe_2O_4$ nanocrystals is shown in Figure 6. Hexagonal nanoparticles are likely templated by the protein localized on hexagonally packed micelles, with the crystal growth along the (111) direction of a cubic cell.

In summary, we have used bioinspired strategies employing a combination of bacterial mineralization proteins and hierarchically self-assembling polymers for room-temperature synthesis of uniform, well-defined $CoFe_2O_4$ nanocrystals that are not found in living organisms. This work provides a highly promising bioinspired route for the controlled synthesis of complex nanomaterials with superior magnetic properties. This pathway of protein-templated synthesis may lead to rational design of nanomaterials for a wide range of applications, from sensing to magnetic data storage to biomedical imaging.

METHODS

Materials and Reagents. All solutions were degassed and sparged with argon prior to their use. Pluronic F127 NF Prill Poloxamer 407 (BASF) was dissolved in toluene, recrystallized from cold hexane, and dried overnight *in vacuo* at room temperature. $CoCl_2 \cdot 6H_2O$ (98%, Aldrich) and $FeCl_2 \cdot 4H_2O$ (99.99%, Aldrich) were transferred to a reaction flask and dissolved in water to form 0.66 and 0.33 M solutions, respectively. Sodium hydroxide, succinic anhydride, Tris-HCl, KCl, *N*,*N*′-dicyclohexylcarbodiimide, diethyl ether, pyridine, *N*-hydroxysuccinimide (NHS), and dichloromethane (Aldrich) were used as received.

The cloning and expression of the full-length recombinant polyhistidine-tagged mms6 protein (*his*-mms6, VGGTIWTGKGLGLGLGLGLGAWGPIILGVVGAGA YAYMKSRDIESAQSDEEVELRDALA, $MW_{calc} \approx 10297$) has been described elsewhere.[23] To minimize the possible influence of the polyhistidine tag and to control protein multimerization, the C-terminal domain of mms6, containing 25 amino acids (*c25*-mms6, YAYMKSRDIESAQSDEEVELRDALA, MW = 2890), was synthesized by GenScript Corp. *c25*-mms6 provides a more compact version of mms6 lacking the hydrophobic N-terminal domain. Its ability to promote shape-specific crystal growth was compared to that of the full-length mms6. Both proteins used in the study were dialyzed against 20 mM Tris-HCl, 100 mM KCl buffer (pH 7.45), which is referred to as the protein buffer.

Activation and Conjugation of F127 Pluronic. The hydroxyl end groups of F127 Pluronic were converted to carboxyl groups by treating it with succinic anhydride in pyridine as reported in the literature.[38] The carboxyl-terminated Pluronic was activated by reaction with NHS at room temperature for 24 h following the procedure reported by Zeng.[39] The NHS-activated Pluronic block copolymer was then covalently bonded (conjugated) with either *his*-mms6 or *c25*-mms6.[39] After vigorous stirring at room temperature for 24 h, the mixture was dialyzed against the protein buffer, using a cellulose ester membrane with a molecular weight cutoff of 12000–14000 (Spectrum Labs), for 48 h at room temperature to remove the unreacted polymer.

Synthesis of Cobalt Ferrite Nanocrystals. Synthesis of $CoFe_2O_4$ nanocrystals was carried out in aqueous solution *via* the oxidative coprecipitation of Fe^{2+} and Co^{2+} using a process reported by Rajendran and co-workers[40] in the presence of the biomineralization proteins described above. The synthesis was carried out in F-127 Pluronic polymeric aqueous gel with reverse temperature gelation in order to slow the diffusion rates, with the biomineralization proteins either unbound or conjugated to the Pluronic triblock copolymer.[23] In the experiments with biomineralization templating agents, 20 μg of unbound *his*-mms6, unbound *c25*-mms6, or *his*-mms6 or *c25*-mms6 conjugated to the functionalized F-127 Pluronic was added to 750 μL of cooled 25% (w/w) F-127 Pluronic aqueous solution. Next, several microliters of the protein buffer solution was added to maintain equal volume and equal protein-to-buffer ratios. Each test tube was charged with 50 μL of 0.66 M $CoCl_2$and 200 μL of 0.33 M $FeCl_2$ solution, to obtain a 1:2 molar ratio of $[Co^{2+}]$:$[Fe^{2+}]$, and 10 μL of 0.0016 M of HCl. To ensure uniform mixing in the F-127 Pluronic, the reaction tubes were incubated at 4 °C for 30 min prior to the reaction. The resulting solution was then brought to room temperature and, under partial argon flow and vigorous stirring, injected with a mixture containing 70 μL of aqueous 1 M NaOH and 11 μL of H_2O_2. The test tubes were charged with an additional 700 μL of NaOH solution under continuous stirring, which resulted in gel dilution and a somewhat lowered viscosity. Nanocrystals were allowed to grow at room temperature for 28 days, after which the precipitated nanocrystals were concentrated at the bottom of the test tube with a magnet, thus ensuring collection of the magnetic fraction of the precipitate. An aliquot of magnetically separated, concentrated suspension was taken for measurements as described below.

The growth of *Magnetospirillum magneticum* strain AMB-1 cells, harvesting, lysing of the bacterial culture, and TEM sample preparation are reported elsewhere.[22]

Materials Characterization. Particle sizes and morphologies of the magnetite and cobalt ferrite samples were examined by using a Tecnai G^2 F20 scanning transmission electron microscope (STEM) at an accelerating voltage of 200 kV. Diluted $CoFe_2O_4$ nanoparticle suspensions were placed on holey carbon-coated copper grids and dried at room temperature. The nature of the obtained $CoFe_2O_4$ powder was verified with powder X-ray diffraction analysis using a Rigaku DMAX diffractometer (45 kV, 20 mA) with graphite-monochromatized Cu $K\alpha$ radiation (λ = 1.54178 Å). Diffractograms were collected at a 2θ–θ step-scan mode of 0.018°/min, with 0.02° step interval. Magnetization measurements were carried out by using a 5T Quantum Design magnetic properties measurement system. The nanoparticle suspension was injected into a polycarbonate capsule and immediately cooled below the freezing temperature of the liquid (~270 K). To compare different samples, the temperature and magnetic field dependence of the magnetization were measured.

Acknowledgment. We thank Dr. Dennis Bazylinski for providing magnetotactic bacteria and useful discussions and Umai Kanapathipillai and Jorge Almodovar for their help in synthesis and materials preparation. T.P., R.P., and P.C.C. acknowledge discussions with Dr. Felis S. Catus. B.N. and S.K.M. acknowledge a useful discussion with Dr. Ram Seshadri. We thank Dr. Matthew J. Kramer and Dr. Yaqiao Wu for assistance with HRTEM. This work was supported by the Department of Energy, Basic Energy Sciences, under Contract No. DE-AC02-07CH11358. R.P. acknowledges partial support from the NSF (grant no. DMR-06-03841) and the Alfred P. Sloan Foundation. D.J. acknowledges financial support from the DOE SULI program. X-ray diffraction measurements were carried out in the Frederick Seitz Materials Research Laboratory Central Facilities, University of Illinois, which is partially supported by the U.S. Department of Energy under grants DE-FG02-07ER46453 and DE-FG02-07ER46471.

REFERENCES AND NOTES

1. Park, J.; An, K.; Hwang, Y.; Park, J.-G.; Noh, H.-J.; Kim, J.-Y.; Park, J.-H.; Hwang, N.-M.; Hyeon, T. Ultra-Large-Scale Syntheses of Monodisperse Nanocrystals. *Nat. Mater.* **2004**, *3*, 891–895.
2. Ditsch, A.; Laibinis, P. E.; Wang, D. I. C.; Hatton, T. A. Controlled Clustering and Enhanced Stability of Polymer-Coated Magnetic Nanoparticles. *Langmuir* **2005**, *21*, 6006–6018.
3. Ai, H.; Flask, C.; Weinberg, B.; Shuai, X.; Pagel, M. D.; Farrell, D.; Duerk, J.; Gao, J. Magnetite-Loaded Polymeric Micelles as Ultrasensitive Magnetic-Resonance Probes. *Adv. Mater.* **2005**, *17*, 1949–1952.
4. Lang, C.; Schuler, D.; Faivre, D. Synthesis of Magnetite Nanoparticles for Bio- and Nanotechnology: Genetic Engineering and Biomimetics of Bacterial Magnetosomes. *Macromol. Biosci.* **2007**, *2007*, 144–151.
5. Bulte, J. M.; Vymazal, J.; Brooks, R. A.; Pierpaoli, C.; Frank, J. A. Frequency Dependence of MR Relaxation Times. II. Iron Oxides. *J. Magn. Reson. Imaging* **1993**, *3*, 641–864.
6. Chiancone, E.; Ceci, P.; Ilari, A.; Ribacchi, F.; Stefanini, S. Iron and Proteins for Iron Storage and Detoxification. *BioMetals* **2004**, *17*, 197–202.
7. Li, M.; Wong, K. K. W.; Mann, S. Organization of Inorganic Nanoparticles Using Biotin-Streptavidin Connectors. *Chem. Mater.* **1999**, *11*, 23–26.
8. Matsunaga, T.; Takeyama, H. Biomagnetic Nanoparticle Formation and Application. *Supramol. Sci.* **1998**, *5*, 391–394.
9. Rousseau, V.; Pouliquen, D.; Darcel, F.; Jallet, P.; Le Jeune, J. J. NMR Investigation of Experimental Chemical Induced Brain Tumors in Rats, Potential of a Superparamagnetic Contrast Agent (MD3) to Improve Diagnosis. *Magn. Res. Mater. Phys. Biol. Med.* **1998**, *6*, 13–21.
10. Tartaj, P.; Gonzalez-Carreno, T.; Ferrer, M. L.; Serna, C. J. Nanotechnology: Metallic Nanomagnets Randomly Dispersed in Spherical Colloids: Toward a Universal Route for the Preparation of Colloidal Composites Containing Nanoparticles. *Angew. Chem., Int. Ed.* **2004**, *43*, 6304–6307.
11. Bazylinski, D. A.; Frankel, R. B. Magnetosome Formation in Prokaryotes. *Nat. Rev. Microbiol.* **2004**, *2*, 217–230.
12. Berry, C. C.; Curtis, A. S. G. Functionalisation of Magnetic Nanoparticles for Applications in Biomedicine. *J. Phys. D: Appl. Phys.* **2003**, *36*, R198–R206.

13. Hernando, A.; Crespo, P.; Garcia, M. A. Metallic Magnetic Nanoparticles. *Sci. World* **2005**, *5*, 972–1001.
14. Lang, C.; Schueler, D. Biomineralization of Magnetosomes in Bacteria: Nanoparticles with Potential Applications. *Microb. Bionanotechnol.* **2006**, 107–124.
15. Reiss, G.; Huetten, A. Magnetic nanoparticles: Applications beyond data storage. *Nat. Mater.* **2005**, *4*, 725–726.
16. Vatta, L. L.; Sanderson, R. D.; Koch, K. R. Magnetic nanoparticles: properties and potential applications. *Pure Appl. Chem.* **2006**, *78*, 1793–1801.
17. Hyeon, T.; Chung, Y.; Park, J.; Lee, S. S.; Kim, Y. W.; Park, B. H. Synthesis of Highly Crystalline and Monodisperse Cobalt Ferrite Nanocrystals. *J. Phys. Chem. B* **2002**, *106*, 6831–6833.
18. Blaskov, V.; Petkov, V.; Rusanov, V.; Martinez, L. M.; Martinez, B.; Munoz, J. S.; Mikhov, M. Magnetic Properties of Nanophase CoFe2O4 Particles. *J. Magn. Magn. Mater.* **1996**, *162*, 331–337.
19. Suslick, K. S.; Price, G. J. Applications of Ultrasound to Materials Chemistry. *Annu. Rev. Mater. Sci.* **1999**, *29*, 295–326.
20. Shafi, K. V. P. M.; Wizel, S.; Prozorov, T.; Gedanken, A. The Use of Ultrasound Radiation for the Preparation of Magnetic Fluids. *Thin Solid Films* **1998**, *318*, 38–41.
21. Prozorov, T.; Prozorov, R.; Shafi, K. V. P. M.; Gedanken, A. Self-Organzation in Ferrofluids Prepared by Sonochemical Irradiation Method. *Nanostruct. Mater.* **1999**, *12*, 669–672.
22. Prozorov, R.; Prozorov, T.; Mallapragada, S. K.; Narasimhan, B.; Williams, T. J.; Bazylinski, D. A. Magnetic Irreversibility and Verwey Transition in Nano-Crystalline Bacterial Magnetite. *Phys. Rev. B: Condens. Matter* **2007**, *76*, 1–10.
23. Prozorov, T.; Mallapragada, S. K.; Narasimhan, B.; Wang, L.; Palo, P.; Nilsen-Hamilton, M.; Williams, T. J.; Bazylinski, D. A.; Prozorov, R.; Canfield, P. C. Protein-Mediated Synthesis of Uniform Superparamagnetic Magnetite Nanocrystals. *Adv. Funct. Mater.* **2007**, *17*, 951–957.
24. Prozorov, R.; Yeshurun, Y.; Prozorov, T.; Gedanken, A. Magnetic Irreversibility and Relaxation in Assembly of Ferromagnetic Nanoparticles. *Phys. Rev. B: Condens. Matter* **1999**, *59*, 6956–6965.
25. Prozorov, R.; Prozorov, T. Effective Collective Barrier for Magnetic Relaxation in Frozen Ferrofluids. *J. Magn. Magn. Mater.* **2004**, *281*, 312–317.
26. Arakaki, A.; Webb, J.; Matsunaga, T. A Novel Protein Tightly Bound to Bacterial Magnetic Particles in Magnetospirillum magneticum Strain AMB-1*. *J. Biol. Chem.* **2003**, *278*, 8745–8750.
27. Bazylinski, D. A. Controlled Biomineralization of Magnetic Minerals by Magnetotactic Bacteria. *Chem. Geol.* **1996**, *132*, 191–198.
28. Anderson, J. A.; Travesset, A. Coarse-Grained Simulations of Gels of Nonionic Multiblock Copolymers with Hydrophobic Groups. *Macromolecules* **2006**, *39*, 5143–5151.
29. Castelletto, V.; Parras, P.; Hamley, I. W.; Baeverbaeck, P.; Pedersen, J. S.; Panine, P. Wormlike Micelle Formation and Flow Alignment of a Pluronic Block Copolymer in Aqueous Solution. *Langmuir* **2007**, *23*, 6896–6902.
30. Foerster, S. Amphiphilic Block Copolymers for Templating Applications. *Top. Curr. Chem.* **2003**, *226*, 1–28.
31. Habas, J.-P.; Pavie, E.; Perreur, C.; Lapp, A.; Peyrelasse, J. Nanostructure in Block Copolymer Solutions: Rheology and Small-Angle Neutron Scattering. *Phys. Rev. E: Nonlin. Soft Matter Phys.* **2004**, *70*, 061802/1061802/8.
32. Ivanova, R.; Lindman, B.; Alexandridis, P. Evolution in Structural Polymorphism of Pluronic F127 Poly(ethylene oxide)–Poly(propylene oxide) Block Copolymer in Ternary Systems with Water and Pharmaceutically Acceptable Organic Solvents: From "Glycols" to "Oils". *Langmuir* **2000**, *16*, 9058–9069.
33. Reynhout, I. C.; Cornelissen, J. J. L. M.; Nolte, R. J. M. Complex Nanostructures from Biohybrid Block Copolymers. *PMSE Preprints* **2006**, *94*, 155–156.
34. Mortensen, K. Structural Studies of Aqueous Solutions of PEO–PPO–PEO Triblock Copolymers, Their Micellar Aggregates and Mesophases; A Small-Angle Neutron Scattering Study. *J. Phys. Condens. Matter* **1996**, *8*, A103–A124.
35. Rill, R. L.; Locke, B. R.; Liu, Y.; van Winkle, D. H. Electrophoresis in Lyotropic Polymer Liquid Crystals. *Proc. Natl. Acad. Sci. USA* **1998**, *95*, 1534.
36. Kurumada, K.; Robinson, B. H. In *Viscosity Studies of Pluronic F127 in Aqueous Solution*; Miguel, M., Burrows, H. D., Eds.; Progress in Colloid Polymer Science 123;Springer: Berlin/Heidelberg, 2004; pp 12–15.
37. Wang, L.; Nilsen-Hamilton, M. Aggregation Studies of the Full-Length mms6 and C-terminal mms6. Manuscript in preparation, 2007.
38. Bali, D. Synthesis of New Gramicidin A Derivatives. *Aust. J. Chem.* **2003**, *56*, 293.
39. Zeng, F. Epidermal Growth Factor-Conjugated Poly(ethylene glycol)-block-poly(valerolactone) Copolymer Micelles for Targeted Delivery of Chemotherapeutics. *Bionconjugate Chem.* **2006**, *17*, 399.
40. Rajendran, M.; Pullar, R. C.; Bhattacharya, A. K.; Das, D.; Chintalapudi, S. N.; Majumdar, C. K. Magnetic Properties of Nanocrystalline $CoFe_2O_4$ Powders Prepared at Room Temperature: Variation with Crystallite Size. *J. Magn. Magn. Mater.* **2001**, *232*, 71–83.